JCI insight

Control of PTH secretion by the TRPC1 ion channel

Marta Onopiuk, … , Leonidas Tsiokas, Kai Lau

JCI Insight. 2020. https://doi.org/10.1172/jci.insight.132496.

Research In-Press Preview Cell biology Endocrinology

Graphical abstract

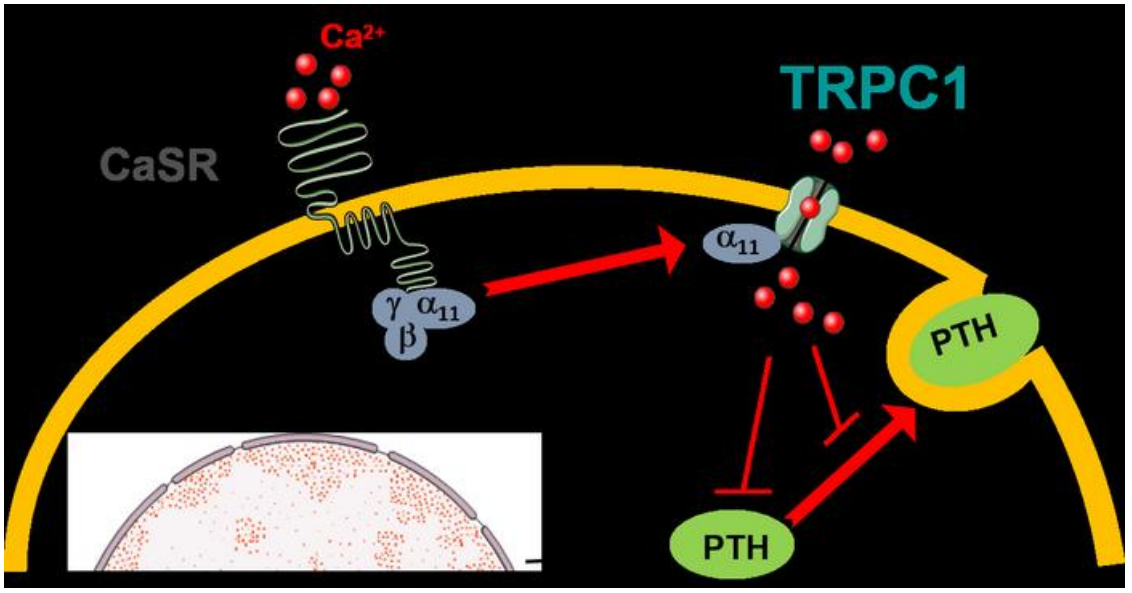

RESEARCH

Control of PTH secretion by the TRPC1 ion channel

Marta Onopiuk[1, a], Bonnie Eby[2, a], Vasyl Nesin[1], Peter Ngo[1], Megan Lerner[3], Caroline M. Gorvin[4, 5], Victoria J Stokes[4], Rajesh V. Thakker[4], Maria Luisa Brandi[6], Wenhan Chang[7], Mary Beth Humphrey[8, 9, b], Leonidas Tsiokas[1, a, b], Kai Lau[2, 9, b].

[1]Department of Cell Biology, University of Oklahoma Health Sciences Center, Oklahoma City, OK 73104, USA

[2]Department of Medicine, Division of Nephrology, University of Oklahoma Health Sciences Center, Oklahoma City, OK 73104, USA

[3]Department of Surgery, Oklahoma City, OK 73104, USA

[4]Academic Endocrine Unit, Radcliffe Department of Medicine, University of Oxford, Oxford, UK

[5]Current institution: Institute of Metabolism and Systems Research and Centre for Membrane Proteins and Receptors, University of Birmingham, Birmingham, UK

[6]Department of Biomedicals Sperimentals and Clinicals Sciences, Università degli Studi di Firenze and Fondazione F.I.R.M.O., Florence, Italy

[7]Department of Medicine, UCSF Endocrinology and Metabolism, UCSF, San Francisco, CA, USA

[8]Department of Medicine, Division of Rheumatology, Immunology, and Allergy, University of Oklahoma Health Sciences Center, Oklahoma City, OK 73104, USA

[9]Department of Veterans Affairs, Oklahoma City, OK 73104, USA

[a]These authors contributed equally

[b] To whom correspondence should be addressed: Kai Lau, address: 825 NE 10th St., Suite 4E, Oklahoma City, OK 73104, telephone number: +1 405-271-8478, email: kai-lau@ouhsc.edu; Leonidas Tsiokas, address: University of Oklahoma Health Sciences Center, 975 NE 10th St., BRC262, Oklahoma City, OK 73104, telephone number: +1 405-271 8001X46211, email: ltsiokas@ouhsc.edu, or Mary Beth Humphrey, address: University of Oklahoma Health Sciences Center, 975 NE 10th St., BRC256, Oklahoma City, OK 73104, telephone number: +1 405-271-7712, email: marybeth-humphrey@ouhsc.edu

The authors declare no conflict of interest

Abstract

Familial Hypocalciuric Hypercalcemia (FHH) is a genetic condition associated with hypocalciuria, hypercalcemia and in some cases inappropriately high levels of circulating parathyroid hormone (PTH). FHH is associated with inactivating mutations in *CaSR* encoding the Ca^{2+} sensing receptor (CaSR), a G protein coupled receptor (GPCR) and *GNA11* encoding G protein subunit alpha 11 (Gα11), implicating defective GPCR signaling as the root pathophysiology for FHH. However, the downstream mechanism by which CaSR activation inhibits PTH production/secretion is incompletely understood. Here, we show that mice lacking the transient receptor potential canonical channel 1 (TRPC1) develop chronic hypercalcemia, hypocalciuria, and elevated PTH levels mimicking human FHH. *Ex vivo* and i*n vitro* studies reveal that TRPC1 serves a necessary and sufficient mediator to suppress PTH secretion from parathyroid glands (PTG) downstream of CaSR in response to high extracellular Ca^{2+} concentration. Gα11 physically interacts with both the N- and C-termini of TRPC1 and enhances CaSR-induced TRPC1 activity in transfected cells. These data identify TRPC1-mediated Ca^{2+} signaling as an essential component of the cellular apparatus controlling PTH secretion in the PTG downstream of CaSR.

Introduction

PTH is a critical hormone for Ca^{2+} homeostasis. In normal conditions, levels of PTH are tightly controlled by serum Ca^{2+} via a negative feedback mechanism in which high serum Ca^{2+} levels suppress the production and/or secretion of PTH from the PTG. This feedback mechanism prevents the development of hypercalcemia or hypocalcemia. In primary hyperparathyroidism often resulting from parathyroid gland (PTG) adenomas, abnormally high levels of PTH result in hypercalcemia, whereas in secondary hyperparathyroidism frequently seen in renal failure elevated PTH levels are actually associated with hypocalcemia. Patients with naturally occurring mutations in *CASR* encoding the Ca^{2+} sensing receptor (CaSR) (1, 2), *GNA11* encoding G protein subunit alpha 11 (Gα11) (3), or *AP2S1* encoding the clathrin-associated adaptor protein-2 sigma subunit 2 (AP2σ2) (4) develop FHH characterized by hypercalcemia and hypocalciuria and is some cases, with inappropriately elevated levels (5). Proteins encoded by the FHH-associated genes function in a linear signaling pathway within the PTG to suppress production and secretion of PTH in response to hypercalcemia. However, an outstanding question has been how hypercalcemia causes the suppression of PTH production and secretion. It has been suggested that a critical step involves a transient rise in intracellular Ca^{2+} concentration in response to high serum Ca^{2+} levels (6, 7). In contrast to most endocrine systems where an increase in intracellular Ca^{2+} concentration triggers exocytosis and hormonal release, the PTG is unique in that an increase in intracellular Ca^{2+} concentration instead suppresses PTH release (7) The molecular identity of the ion channels mediating this transient increase in intracellular Ca^{2+} concentration driving the suppression of PTH release has been unknown. Therefore, identification of these channels and the mechanisms underlying CaSR-induced Ca^{2+} signaling suppression of PTH secretion is of paramount importance in understanding and treating pathological conditions resulting from abnormal PTH levels.

CaSR is coupled to three subclasses of G proteins, Gα11/αq, Gαi/o, and Gα12/13 (8, 9). The identification of *GNA11* as an FHH-associated gene and further functional and genetic studies on Gα11 indicate that the coupling of CaSR to Gα11 may be directly linked to the suppression of PTH production

and/or secretion. Activation of Gα11/αq-coupled CaSR leads to the generation of inositol trisphosphate (IP_3), which triggers Ca^{2+} release from endoplasmic reticulum (ER) and stimulation of Ca^{2+} influx from the extracellular fluid mediated by store- and/or receptor- operated Ca^{2+} entry (SOCE or ROCE) channels, localized at the plasma membrane. SOCE channels are defined as the channels activated exclusively via the depletion of the intracellular Ca^{2+} stores following the activation of any pathway that involves the generation of IP_3 as a second messenger and involve the ER Ca^{2+} sensor, stromal interaction molecule 1 (STIM1), and the pore-forming subunit, Orai1 (10). ROCE channels are activated via intermediaries generated during the activation of cell surface receptors and nearly all of the 28 known TRP channels can function as ROCE channels, depending on cell- and tissue- contexts (11, 12). Therefore, theoretically both SOCE and ROCE channels can be activated following the stimulation of the CaSR. TRPC1 belongs to the canonical subgroup of TRP channels and has been implicated in both SOCE and ROCE (13). TRPC1 can be activated by CaSR in rabbit mesenteric arteries (14), colonic epithelial (15, 16), endothelial (17), and breast cancer cells (18), making it an ideal candidate for mediating the suppression of PTH secretion downstream of CaSR in the PTG.

Using a combination of *in vivo*, *ex vivo*, and *in vitro* approaches, our studies show that TRPC1 functions downstream of CaSR in the suppression of PTH secretion and *Trpc1*-null mice show an FHH-like phenotype. However, its mechanism of activation does not involve store depletion, but instead a protein-protein interaction with Gα11, a protein directly coupled to CaSR and genetically implicated in FHH. Thus, our study identifies TRPC1 as one of the ion channels mediating the mechanism by which high Ca^{2+} serum levels suppress PTH secretion.

Results

Trpc1$^{-/-}$ mice develop FHH Global *Trpc1$^{-/-}$* mice have been described (19). Homeostatic serum Ca^{2+} levels were significantly higher in male or female *Trpc1$^{-/-}$* mice in 7 months of age **(Figure 1A)**. Hypercalcemia was observed as early as in 3.5 and persisted up to 21.5 months in age-matched null littermate males (11.31 ± 0.28 mg/dl in *Trpc1$^{-/-}$* vs 9.92 ± 0.41 mg/dl in *Trpc1$^{+/+}$*, $p<0.05$) **(Figure S1A)**. *Trpc1$^{+/-}$* male mice exhibited significant hypercalcemia **(Figure S1B)** suggesting that heterozygous deletion of *Trpc1* is sufficient to produce a hypercalcemic phenotype. PTH levels were significantly higher in 7-month-old homozygous mutant males and inappropriately high in 7-month-old homozygous mutant females (since it was not suppressed by hypercalcemia as expected in normal physiology) **(Figure 1B)**. Inappropriately high PTH was observed in younger and older mice **(Figure S1C)**. Hypercalcemia in *Trpc1$^{-/-}$* mutant male or female mice was present in either fasted (10 h prior to blood collection) or animals allowed to feed *ad lib*, arguing against increased gut Ca^{2+} absorption as the mechanism for the hypercalcemia in mice lacking *Trpc1* **(Figure S1D)**. Despite hypercalcemia, 24 h urine Ca^{2+} excretion **(Figure 1C)**, renal Ca^{2+} clearance **(Figure 1D),** and urine Ca^{2+}/creatinine ratio were all reduced in 7-month-old *Trpc1$^{-/-}$* males and females **(Figure 1E).** Reduced urine Ca^{2+} clearance persisted up to 21.5 months (5.8 ± 3.4 μl/min in *Trpc1$^{-/-}$* males vs 29.3 ± 7.9 μl/min in *Trpc1$^{+/+}$* males). Serum Mg^{2+}, renal Mg^{2+} clearance, urine Mg^{2+} excretion, and 24h urine Mg^{2+}/creatinine ratio were unaffected by deletion of *Trpc1* **(Table 1)**. These data indicate that *Trpc1$^{-/-}$* mice are hypocalciuric and overall, they show the classic triad of FHH of hypocalciuria, hypercalcemia and significantly elevated or inappropriately high levels of circulating PTH.

To evaluate if these phenotypes were secondary to renal disease and/or disorders of vitamin D metabolism, we measured serum levels of 1,25 $(OH)_2$ vitamin D, creatinine, and calcitonin. 1,25 $(OH)_2$ vitamin D was unchanged in 7 month- old males **(Table 1)**. Similarly, serum creatinine was similar to WT in 1-year-old mice **(Table 1)**. Creatinine clearance in *Trpc1$^{-/-}$* mice was comparable to WT mice **(Table**

1), indicating that renal failure could not have accounted for the hypercalcemia and elevated PTH levels seen in *Trpc1*$^{-/-}$ mice. Serum phosphorus levels in *Trpc1*$^{-/-}$ mice were similar to *Trpc1*$^{+/+}$ mice **(Table 1)**. Hematocrits were not different at 8.5 months of age and lower at 10.5 months and 21.5 months, showing that hemoconcentration was not responsible for the hypercalcemia **(Table 1)**. Plasma levels of calcitonin, another regulator of serum Ca^{2+}, were unchanged in 7- month-old *Trpc1*-null males **(Table 1)**, suggesting that deletion of *Trpc1* does not affect calcitonin secretion from C cells of the thyroid gland that could indirectly influence serum Ca^{2+} and/or PTH secretion.

Despite high PTH levels seen in primary hyperparathyroidism typically being associated with low bone mass and osteoporosis, FHH patients manifest slightly reduced, normal or even increased bone mass (20, 21). Mildly increased bone mass is also seen in mice lacking the CaSR in the PTG (22). Our previous work has shown that 12-week-old male *Trpc1*$^{-/-}$ mice have slightly increased bone mass (23). We extended the analysis to 19-month-old animals and found that *Trpc1*$^{-/-}$ mice had 83% increase in bone volume to tissue volume, 27% reduction in trabecular spacing, 36% increase in trabecular number and 181% increase in connectivity density **(Figure S2 A-D)**.

TRPC1 mutations not detected in patients with FHH The phenotype of the *Trpc1*$^{-/-}$ mice is consistent with that of FHH in humans, and the possibility that mutations in the *TRPC1* gene may be a cause of hypercalcemia in some FHH patients who did not have *CASR*, *GNA11* or *AP2S1* mutations, was therefore explored. Sanger DNA sequence analysis (14 patients) or whole exome sequencing (5 patients) did not detect any point mutations, deletions, insertions, or unreported SNPs. However, a 16bp segment corresponding to the 5'UTR in short form of TRPC1 or amino acid residues VGAGG in long form of TRPC1 (**Figure S3**) could not be reliably ascertained due to repetitive elements. A binomial analysis predicted that the use of 19 samples in total would have a greater than 95 and 98% likelihood of detecting at least one TRPC1 mutation, assuming a mutation prevalence of 15% and 20% respectively (24). Whole

exome sequencing did identify a common polymorphism (p.A14T, present in 7490 out of 261160 alleles in the gnomAD v2.1.1 database) in one FHH patient.

TRPC1 is required for the suppression of PTH secretion in isolated mouse parathyroid glands TRPC1 was widely expressed in WT, but not in mutant PTGs **(Figure 2A)**. To test for a PTG-autonomous effect of TRPC1 on PTH secretion, we determined the secretory capacity of isolated PTGs from both groups of 14-week-old male and female mice, as was done previously for the CaSR (22). Males and females had similar PTH secretion maximum (Rmax) and minimum (Rmin) as well as Ca^{2+} set points; therefore, we pooled the data to increase the power of the analysis. Absolute Rmax values were ~3-fold higher in *Trpc1*$^{-/-}$ compared to *Trpc1*$^{+/+}$ PTGs **(Figure 2B)** accompanied with a significant rightward shift in the Ca^{2+} set point from 1.04 ± 0.15 mM in *Trpc1*$^{+/+}$ mice to 1.25 ± 0.08 mM in *Trpc1*$^{-/-}$ mice **(Figure 2C)**. These *ex vivo* effects were more severe than the deletion of one allele of *Casr* in the PTG of 3-month-old mice, but less severe than the deletion of two *Casr* alleles (22, 25), suggesting that TRPC1 may significantly contribute (by more than 50%) to the effects of CaSR in the secretion of PTH from the isolated PTG.

Parathyroid cells depleted of TRPC1 secrete more parathyroid hormone Derived from rat PTG, PTH-C1 cells express CaSR, produce and secrete PTH and are currently the only known cell line available for studying PTH secretion in rodents (26). Using CRISPR/Cas9 gene editing, we introduced a frame-shift in the *Trpc1* locus in PTH-C1 cells and generated several stable clones. One of these clones, PTH-C1$^{Trpc1\text{-KO}}$ **(Figure S4A and S4D)** was used for functional PTH secretion assays. Deletion of TRPC1 led to a 44% increase in secreted PTH (from 8.7 ± 0.8 pg/ml in wild type cells to 12.6 ± 1.2 pg/ml in PTH-C1$^{Trpc1\text{-KO}}$ cells) in the presence of low extracellular Ca^{2+} concentration (0.5 mM Ca^{2+}) which should promote PTH secretion **(Figure 3A)**. Similar effects were seen when PTH-C1 cells were treated with Pico145, a specific inhibitor of TRPC1/TRPC4/TRPC4 channels (27) **(Figure S5A)**. RT-PCR failed to

detect TRPC4 or TRPC5 mRNAs in PTH-C1, indicating that Pico145 increased PTH secretion most likely by inhibiting endogenous TRPC1 in these cells **(Figure S5B)**.

To examine whether endogenous TRPC1 controls PTH secretion rather than gene expression, we generated and characterized stable clones overexpressing mouse PTH using a heterologous promoter (CMV) that should not be affected by TRPC1 levels. Two individual clones highly expressing PTH (PTH-C1$^{Pth\text{-}1}$ ~20,000 fold and PTH-C1$^{Pth\text{-}2}$ ~2,000-fold compared to parental PTH-C1 cells) were subsequently transfected with a TRPC1-specific CRISPR/Cas9 construct and two individual clones (PTH-C1$^{Pth\text{-}1/Trpc1\text{-}KO}$ and PTH-C1$^{Pth\text{-}2/Trpc1\text{-}KO}$) with complete deletion of TRPC1 (verified by Sanger sequencing of the recombination site at the *Trpc1* locus, **Figure S4B-C)** were used for functional assays. PTH-C1$^{Pth\text{-}1/Trpc1\text{-}KO}$ cells secrete 50.9 ± 2.7 ng/ml PTH, which was 106% higher than PTH-C1$^{Pth\text{-}1}$ cells (24.8 ± 2.0 ng/ml) **(Figure 3B)**. Similarly, PTH-C1$^{Pth\text{-}2/Trpc1\text{-}KO}$ cells showed 85% higher PTH secretion (4,574 ± 48 pg/ml) than PTH-C1$^{Pth\text{-}2}$ cells (2,473 ± 53 pg/ml) **(Figure 3C)**. Transfecting back wild type TRPC1α suppressed PTH secretion by 31% in PTH-C1$^{Pth\text{-}2/Trpc1\text{-}KO}$ cells **(Figure 3E)**. However, transfection of TRPC1α F689A, with a single amino acid mutation in its pore region **(Figure 3D)** that reduces Ca^{2+} permeability (28) and CaSR-induced Ca^{2+} influx **(Figure 3F),** failed to suppress PTH secretion (0.7%) in these cells **(Figure 3E)**. In the presence of mutant TRPC1αF689A, spermine activation of CaSR induced less intracellular Ca^{2+} accumulation than PTH-C1 cells co-expressing CaSR and wild type TRPC1α **(Figure 3F)**. These data show that TRPC1α has an essential and specific role in suppressing PTH secretion in PTH-C1 cells and this property involves its ability to conduct Ca^{2+}.

TRPC1 overexpression suppresses PTH secretion Next, we determined whether TRPC1 overexpression can suppress PTH secretion in PTH-C1 cells. Overexpression of wild-type TRPC1α, but not TRPC1αF689A, suppressed PTH secretion in PTH-C1 cells **(Figure 4A)**. We also compared side-by-side overexpression of CaSR (positive control) and two other highly expressed TRP channels in the

PTG, TRPM4 or TRPM7 **(Figure 4B)**, or wild type STIM1, Orai1 and their constitutively active mutants, STIM1R304W and Orai1P245L (29). We chose to test the effect of wild type and active mutants of STIM1 and Orai1 on PTH secretion because we had shown earlier that TRPC1 functions together with these proteins to increase the dynamic range of store-operated Ca^{2+} entry channels (23). Overexpression TRPC1α or CaSR suppressed PTH secretion **(Figure 4A)**. Overexpression of TRPM4, TRPM7, STIM1, or Orai1 had no effect on PTH secretion, whereas overexpression of constitutively active STIM1 or Orai1 mutants increased PTH secretion. Knockdown of Orai1 did not affect PTH secretion. The positive effect of constitutively active STIM1/Orai1 mutants on PTH release is consistent with the well-known role of store-operated Ca^{2+} entry channels in hormonal release, exocytosis, and mast cell degranulation (30). These data provided additional evidence that TRPC1 has a specific, essential, and sufficient role in suppressing PTH secretion in PTH-C1 cells, and does so independently of its ability to enhance store-operated Ca^{2+} entry.

TRPC1 functions downstream of CaSR in PTH-C1 or HEK293 cells To test whether TRPC1 functions downstream of CaSR in Ca^{2+} signaling in PTH-C1 cells, we transiently depleted TRPC1 in PTH-C1 cells using a rat *Trpc1*--specific siRNA. *Trpc1* mRNA translation is initiated by two alternative start sites. Translation initiation by an upstream leucine (L) generates the long form of TRPC1, whereas initiation by a downstream methionine (M) generates the short form of TRPC1. The two isoforms differ by N-terminal extension of 78 amino acids (23). PTH-C1 cells expressed predominantly the long form of TRPC1, which was downregulated in cells transfected by a rat *Trpc1*-specific siRNA **(Figure 5A)**. Depletion of TRPC1 attenuated intracellular Ca^{2+} signaling in cells activated by extracellular Ca^{2+}, Spermine or R-568 **(Figure 5B-E)**, which are all well-established activators of the CaSR (9). The response to Spermine represented specific activation of CaSR, since it was completely blocked in the presence of the CaSR-specific inhibitor, NPS2143 **(Figure 5D)**. These data showed that TRPC1 depletion reduced CaSR-induced Ca^{2+} signaling, consistent with the hypothesis that TRPC1 functions downstream of CaSR activation to increase intracellular Ca^{2+} concentration to suppress PTH secretion. Activation of CaSR can lead to the

concurrent activation of both store-operated and receptor-operated Ca^{2+} entry channels. Our functional PTH secretion assays suggested that TRPC1 functions independently of SOCE channels in suppressing PTH secretion. Here, we used a heterologous system to test whether TRPC1 can be specifically coupled to CaSR and function independently of SOCE channels in Ca^{2+} signaling. To test for the contribution of TRPC1 in store-operated Ca^{2+} entry, HEK293 cells were transfected with TRPC1 and CaSR or m1 acetylcholine receptor (AchR), which is also coupled to Gα11/Gαq, and stimulated with thapsigargin to deplete internal Ca^{2+} stores followed by direct activation of transfected CaSR or m1 AchR with Spermine or Carbachol, respectively. Expression of TRPC1 enhanced Ca^{2+} signaling in cells transfected with CaSR **(Figure 5F)**, but not m1 AchR **(Figure 5G)**. In addition, overexpression of TRPC1 did not have an effect on thapsigargin-induced Ca^{2+} signaling. These data suggest that TRPC1 is coupled to CaSR via a mechanism independent of depletion of intracellular Ca^{2+} stores, supporting our data from PTH secretion assays in PTH-C1 cells, in which overexpression or knockdown of STIM1 or Orai1 did not affect PTH secretion.

Gα11 physically interacts with TRPC1 and increases its activity Given the established role of Gα11 in FHH and PTH secretion (3), we asked whether Gα11 overexpression could further enhance CaSR-induced TRPC1-mediated Ca^{2+} influx. Indeed, overexpression of Gα11 augmented TRPC1-mediated Ca^{2+} influx in response to Spermine activation of CaSR in HEK293 cells using two different protocols **(Figure 6A and B)**. Gα11 could enhance TRPC1 activity by multiple mechanisms. One possible mechanism could involve complex formation of Gα11 with TRPC1, as previously reported for receptor-activated TRP channels and $G\alpha_q$ (31). Therefore, we examined whether Gα11 could interact with TRPC1. We tested both long and short forms of TRPC1α and TRPC1ε isoforms. TRPC1α is the most widely expressed form of TRPC1, whereas TRPC1ε has a 7 amino acid deletion at the beginning of exon 5 corresponding to the N-terminal cytosolic domain of TRPC1 and so far, is shown to be expressed in myeloid precursor cells (23). Co-immunoprecipitation experiments in transiently transfected HEK239T

cells followed by deletion analysis showed either TRPC1α or TRPC1ε isoforms interacted with Gα11 through their N- and C-termini **(Figure 6C-D)**. Consistently, endogenous TRPC1 co-localized with Gα11 in PTH-C1 cells **(Figure S6)**. In contrast, TRPC1 did not interact with Gαs, showing specificity of TRPC1 to Gα11 **(Figure 6C-D)**. In light of genetic data in which inactivating mutations in *GNA11* in humans produce a phenotype also seen in *Trpc1*-null mice, plus the molecular and functional data that Gα11 co-immunoprecipitates and enhances the activity of TRPC1, we propose that the direct interaction between TRPC1 and Gα11 potentiates the stimulatory effects of CaSR on TRPC1.

Discussion

The discovery of CaSR had a profound impact on our understanding how PTG cells sense extracellular Ca^{2+} levels (2, 6, 9, 32, 33). However, there are still gaps in our knowledge regarding how PTG cells regulate PTH secretion downstream of CaSR. We provide *in vivo, ex vivo,* and *in vitro* evidence that TRPC1 functions downstream of CaSR to suppress PTH secretion. This information can help direct future studies to better understand how Ca^{2+} signaling can regulate PTH release, calcitonin secretion, and secretion of other hormones from cells with a functional CaSR.

Global deletion of *Trpc1* resulted in a phenotype that showed significant similarities to FHH (21, 34). Statistically as a group, FHH patients exhibit mild but significant hypercalcemia, while a few of them show elevated PTH (5, 35), similar to male *Trpc1*$^{-/-}$ mice. Hypocalciuria, a hallmark of FHH not typically seen in primary hyperparathyroidism (5, 36), is also observed in our *Trpc1*$^{-/-}$ mice. These data are consistent with the idea that TRPC1 functions downstream of CaSR in the PTG and the kidney. Unchanged 1,25 $(OH)_2$ vitamin D levels are observed in FHH patients (34, 37, 38), which is corroborated in our *Trpc1*$^{-/-}$ mice. A few differences are noteworthy between *Trpc1*$^{-/-}$ mice and FHH patients. Serum Mg^{2+} is often moderately increased in some FHH patients (3, 4, 39), but Mg^{2+} levels were normal in *Trpc1*$^{-/-}$ mice. Second, *Trpc1*$^{-/-}$ mice and mice with kidney-specific deletion of *Casr* have normal serum phosphorous levels (40), unlike FHH patients with reduced levels (35). Finally, there are changes in skeletal manifestation between our mice and FHH patients. In FHH, bone mass is generally comparable to normal controls (20, 21, 41). However, our *Trpc1*-null mice have significantly increased and progressive changes in bone mass with age. Indeed, previously we reported significantly decreased osteoblast number per bone surface and reduced osteoclast numbers per bone surface in histomorphometric assays of 3-month-old *Trpc1*-null mice (23). These similarities and differences may correlate to compensatory proteins that differ between mouse and man in the kidney, parathyroid gland and bone cells. With the exception of *Casr*$^{+/-}$ mice (42) and a newly described mouse model carrying a loss-of-function mutation (D195G) in

Gna11 (43), which recapitulate human FHH both at the disease phenotypic and genetic levels, there are no other suitable mouse models for FHH including orthologous mouse models. For example, while dominant loss-of-function mutations in *GNA11* result in FHH in patients (3), homozygous global deletion of *Gna11* in the mouse did not produce a significant phenotype (44). The PTG-specific deletion of *Gnaq* combined with global deletion of *Gna11* recapitulated some aspects of FHH in the mouse (45), suggesting potential gene redundancy by *Gnaq* in the mouse, but not in man. Alternatively, dominant negative effects of loss-of-function alleles of *Gna11* could be implicated in FHH. Nevertheless, the generation of additional mouse models of FHH could help advance our understanding of the pathophysiology of FHH and diseases of the PTG. We believe that the global *Trpc1* knockout mouse model presented here can be considered as a suitable mouse model for FHH because it recapitulates several key features of FHH. Additional refinements could be made by the tissue-specific deletion of *Trpc1* in the PTG, bone, and kidney.

Our data suggest that Gα11-mediated signaling downstream of CaSR couples serum Ca^{2+} concentration and PTH secretion. CaSR is linked to several classes of Gα subunits and it remains unknown which subclass(es) and how specific G protein(s) mediate the CaSR's effects on PTH secretion (9). The identification of naturally occurring mutations in *GNA11* in patients with FHH2 strongly suggests that the Gα11/αq subclass conveys the signal to suppress PTH secretion following activation of CaSR (3). Our data support this hypothesis and further identify the ion channel mediating such an effect. While we favor the idea that TRPC1 is a direct target of activated Gα11, we cannot rule out a possible modulation of TRPC1 activity by other Gα subclasses coupled to CaSR, either directly via protein-protein interactions or indirectly via cAMP/PKA-mediated signaling (Gαi/o) and regulation of the actin cytoskeleton (Gα12/13). The FHH-like phenotype we observed in *Trpc1*-null mice is less severe than the phenotype produced by the deletion of CaSR in mice (22, 42), suggesting that loss of TRPC1 in the PTG produces a milder phenotype than the loss of CaSR signaling. While other Gα11-activated Ca^{2+}-permeable channels can work in parallel with TRPC1 to suppress PTH secretion, Ca^{2+}-independent signaling could

also account for the remaining effect of PTH suppression in *Trpc1*-null cells/tissues. Alternatively, TRPC1-mediated Ca^{2+} signaling may have a permissive role in the suppression of PTH secretion under conditions of abnormally high serum Ca^{2+} levels. Regardless of the exact mechanism by which TRPC1 influences PTH secretion and the extent to which it contributes to the overall effect of CaSR on PTH secretion, our studies identify the first ion channel that can function downstream of CaSR in the control of PTH secretion and thus, can spur new studies on the role of Ca^{2+} signaling in PTH homeostasis.

While TRPC1 was the first mammalian TRP channel identified more than 20 years ago (46), its activation mechanism remains unclear (13). Our studies identifying TRPC1 as part of the cellular apparatus controlling PTH secretion have implications in its activation mechanisms. We had shown earlier that TRPC1 can be activated by store depletion (23), but our PTH secretion data in PTH-C1 cells show that activation by store depletion could not account for its effect on PTH secretion. This conclusion is based on PTH secretion data whereby overexpression or depletion of STIM1 or Orai1 did not affect PTH secretion in PTH-C1 cells and furthermore, overexpression of constitutively active STIM1 and Orai1 identified in patients with Stormorken or a Stormorken-like syndrome, respectively, enhanced rather than suppressed PTH secretion. While this seems to be at odds with mild hypocalcemia reported in some Stormorken patients (47), it is in agreement with the well-established role of SOCE channels in exocytosis and hormonal release (30). The hypocalcemia seen in Stormorken patients could be due to secondary effects of STIM1R304W in tissues other than the PTG, such as the kidney or bone. More studies are necessary to determine the effect of STIM1R304W or Orai1P245L on hypocalcemia.

We show that overexpression of $G\alpha 11$ increases TRPC1-mediated Ca^{2+} influx and $G\alpha 11$ physically interacts with both the N- and C-terminus of TRPC1. We propose that TRPC1 can be directly activated by a physical interaction with $G\alpha 11$. Our data do not favor the idea that freed $G\beta\gamma$ complex mediates an effect on TRPC1, because inhibition of $G\beta\gamma$ complex with Gallein did not affect PTH secretion in PTH-C1 cells (unpublished observation). Direct $G\alpha q$-mediated regulation of TRP channels was first described in

Drosophila TRPL channel (31), which shows the closest homology to members of the TRPC subgroup of mammalian TRP channels. Recently, TRPC4 or TRPC5 was shown to physically interact with Gαq, which is structurally related to Gα11 (48). We have shown that TRP channels including the canonical group (TRPC1-7) require an intramolecular interaction between their N- and C-termini during activation (49). This intramolecular interaction is influenced by levels of membrane phospholipid, PIP_2 and mediated by a tryptophan (W) residue in the Pre-S1 domain and an arginine (R) residue in the TRP-box domain in the C-terminal tail. It would be interesting to know whether interaction of TRCP1 and Gα11 involves these domains. Nevertheless, because Gα11 interacted with both the N- and C-terminus of TRPC1 and overexpression of Gα11 increased TRPC1 activity, we speculate that a physical interaction with Gα11, following PIP_2 breakdown would stabilize the N-/C-interaction causing faster activation of TRPC1.

In summary, our data identify TRPC1 as one of the channels mediating a critical step in the suppression of PTH secretion in response to a rise in serum Ca^{2+}. Information generated by our studies can be useful in designing new and more effective therapeutic approaches for diseases of the PTG by targeting molecules downstream of CaSR.

Materials and Methods

Mice

Mice were maintained under pathogen-free condition in the barrier facility of University of Oklahoma Health Sciences Center. All procedures were approved by the Institutional Care and Use Committee of University of Oklahoma Health Sciences Center. Wild type (*Trpc1*$^{+/+}$) and *Trpc1*$^{-/-}$ mice were on a pure 129/SvEv background (19).

Cell culture

PTH-C1 cells, cell line derived from rat PTG, were the generous gift of Dr. Maria Luisa Brandi (FirmoLab, Università degli Studi di Firenze) and cultured in prescribed conditions (26). HEK293 and HEK293T cells were purchased from American Type Culture Collection (ATCC) and cultured in Dulbecco's modified Eagles medium (DMEM) [Corning; 10-013] enriched by 10% FBS [Atlanta Biologicals; S11550].

In vivo studies

Collection of blood, urine, and clearance samples

Mice were weighed every 7-10 days. Studies were performed on mutant (*Trpc1*$^{-/-}$) and littermate controls (*Trpc1*$^{+/+}$) from 3.5 to 21.5 months of age. Twenty four-hour urine was collected at various times through 21.5 months in individual metabolic cages. Trace amount of sugar was added to drinking water to promote ingestion and to increase urine volume in order to optimize the completeness of collection, as verified by daily creatinine excretion. Water and food intake was monitored during the balance studies. Blood was collected by tail bleed, fasted or unfasted whichever appropriate, periodically from age 7 through 21.5 months, usually synchronized with metabolic urine collections as appropriate. Renal clearance was performed in individual mice at 21.5 months to measure Ca^{2+} in urine directly collected from urinary

bladder via indwelling catheters and to measure glomerular filtration rate by intravenously infused inulin using methods we established as described earlier (50).

Measurements of creatinine, Ca^{2+}, and Mg^{2+} in urine and blood and analysis of blood PTH, Calcitriol and Calcitonin.

Creatinine was measured by HPLC (Buck Scientific, CT). Ca^{2+} was measured using Ca Arsenazo III dye adapted for a plate reader (Pointe Scientific, MI). Mg^{2+} was measured using Arsenazo dye (Thermo Scientific-Fisher, VA). PTH was measured using a Mouse PTH 1-84 ELISA kit (Immunotopics, CA). Mouse Calcitriol (or 1,25-dihydroxyvitamin D) and Calcitonin were measured using an ELISA (Mybiosource, Ca).

RNA interference

PTH-C1 cells were cultured to 70% confluency and transfected with siTRPC1 [L-080128-02-0005 Dharmacon] or siOrai1 [L-081151-02-0005 Dharmacon] or non-targeting siRNA [D-001810-10-05 Dharmacon] using Lipofectamine3000 (Invitrogen). Two days after transfection cells were transferred into 24-well plates for PTH secretion analysis or 18 mm glass disks for single cell Ca^{2+} imaging analysis.

CRISPR/Cas9

Exon 1 of the rat *Trpc1* locus was edited using CRISPR/Cas9 and the following guide: (T2) 5'-CACCGGGCGCTGAAGGATGTGCGAG-3' or (T3) 5'-CACCGGGCGGCCCTGTACCCGAGCA-3'. The *Trpc1*-specific sgRNA (T2) was cloned into lentiCRISPRv2 puro vector (Addgene) and used to transfect PTH-C1 cells. Puromycin-resistant stable clones were obtained, expanded, gene editing of the *Trpc1* locus was determined by Sanger sequencing.

Patients and DNA sequence analysis

Informed consent was obtained from individuals using protocols approved by the local and national ethics committees (MREC/02/2/93). Nineteen unrelated FHH patients in whom previous mutational analysis of CASR, GNA11, and AP2S1 genes by Sanger DNA sequencing, had not identified any abnormalities of the coding regions and exon-intron boundaries, were ascertained. DNA sequence analyses, using Sanger sequencing, of TRPC1 exons 1-12 of transcript ENST00000273482 and their adjacent splice sites were performed using leucocyte DNA and gene-specific primers (Sigma-Aldrich) (**Table S1**), as previously reported (24). WES was performed using leucocyte DNA, as previously described (4). Publicly accessible databases, including dbSNP (http://www.ncbi.nlm.nih.gov/projects/SNP/), 1000 genomes (http://browser.1000genomes.org), the National Heart, Lung and Blood Institute (NHLBI) Exome Sequencing Project (http://evs.gs.washington.edu/EVS/, EVS data release ESP6500SI) representing the exomes of approximately 6500 individuals, and the gnomAD v2.1.1 database (gnomad.broadinstitute.org) representing 125,748 exomes and 15,708 genomes of unrelated individuals mapped to the GRCh37/hg19 reference sequence, were examined for the presence of sequence variants.

Expression plasmids

Mouse PTH [MR200486] and Gnα11 [MR205495] cDNAs were purchased from Origene. Human Orai1 [BC015369], mouse STIM1 [BC021644], mouse TRPC1α or TRPC1ε [CA327829] were obtained from Open Biosystems as described earlier (23). TRPM4 and TRPM7 cDNAs were obtained from Dr. A. Scharenberg (University of Washington, USA).

Single cell Ca^{2+} imaging

Fura2/AM labeling- PTH-C1 cells were plated onto glass coverslips and loaded with 2 μM Fura-2/AM in extracellular solution (ECS) containing 140 mM NaCl, 5 mM KCl, 1 mM $MgCl_2$, 1.8 mM $CaCl_2$, 10 mM glucose, and 15 mM Hepes, pH 7.4, ($[Ca^{2+}]_o$: 1.8 mM) in the presence of 0.05% Pluronic F-127 for 45

min at room temperature. Cells were washed twice in ECS and incubated for 15 min in 37° C before intracellular imaging. Cells were incubated in ECS (Figure 5B and C) or a Ca^{2+}-free solution (same as ECS but without $CaCl_2$) (Figure 5D) and stimulated with extracellular Ca^{2+} (Figure 5B) or Spermine (Figure 5C and D) at the indicated times. Individual cells were excited by the DeltaRam X™ monochromator (Photon Technology International) and emission images were collected by a high definition imaging (HDI) scientific CMOS camera driven by the EasyRatioPro software (Photon Technology International). Fluorescence ratios of 340/380 were taken every 5 s using 30 ms exposure time. Intracellular Ca^{2+} concentration was expressed as 340/380 ratio.

GCaMP3 labeling- PTH-C1 (Figure 6E) or HEK293 cells (Figs. 3F, 5F and G, and Figure 6A and B) were transfected with GCaMP3. Two days after transfection, cells were processed for single cell Ca^{2+} imaging as described for Fura2/AM-labeled cells, but excitation was set at 474 nm and emission at 510 nm. Fluorescence intensity was acquired every 5 sec for 100 msec and intracellular Ca^{2+} concentration was expressed as the ratio of fluorescence signal at any given time point over baseline fluorescence (F_0, average fluorescence intensity before the addition of drug) (F/F_0).

Ex vivo secretion of PTH

Sixteen week-old mice were euthanized and parathyroid glands were extracted. PTH secretion was performed as described (23). Glands were immediately transferred into 500 μl of inhibition buffer solution (3 mM Ca^{2+}, 0.5 mM Mg^{2+}, 0.2% BSA, 20 mM HEPES/MEM-EBSS-CMF, pH 7.4) and kept on ice. Next, glands were transferred onto 0.1 μM Nucleopore Track-Etch Membrane [Whatman; 110405] and equilibrated in inhibition solution for 1h in a 37°C/5%CO_2 incubator. Membranes with glands were transferred in buffer solutions (500 μl) containing 0.5, 0.75, 1, 1.25, 1.5, 2, or 3 mM Ca^{2+} for 30 min. Secreted PTH was determined using the Mouse PTH 1-84 ELISA Kit [60-2305] from Immutopics.

In vitro secretion of PTH

Secreted PTH from native and transiently or stably transfected PTH-C1 cells was determined using a Rat Intact PTH ELISA Kit [Immutopics; 60-2500]. PTH was collected after 4h incubation in fresh secretion media solution (0.5 mM Ca^{2+}, 0.5 mM Mg^{2+}, 0.2% BSA, 20 mM HEPES/MEM-EBSS-CMF, pH 7.4) prior to quantification of PTH.

PCR

PTH-C1 cells were collected in TRIzol [Invitrogen; 15596026]. RNA isolation was performed according to the manufacturer's instructions. Five μg of RNA was used for reverse transcription. mRNA was combined with oligo (dT) 12-18 primer [Invitrogen; 18418012] and random hexamers [Invitrogen; N8080127] and incubated for 10 min in 70°C. Next, 5X buffer, 0.5 μM dNTP, 10 mM DTT and 20U/μl of SuperScript III were added [reverse transcription kit 18080093 from Invitrogen] and reaction was performed under the following conditions: 42°C for 45min, 52°C for 30min and 70°C for 15min. Primers used for further PCR: TRPC1 Fw: GAGTTACCTTCGGCTCTTCTTT, Rev: GCTGAGGCTGCTGATCATATAG, nested Fw: GCTCTGTTCTGGTACATCTTCTC, Rev: GGCAGTGTGCATTTGTCATC; TRPC4 Fw: GAATGCTCCTGGACATCCTAAA, Rev CCTCATCACCTCTTGGTATTGG, nested Fw GGTTAAGCTGCAAAGGCATAC, Rev CCAAAGCTTTCTGGCTTTCTTC; TRPC5 Fw CAAGGTCCCGACTGAACATATAC, Rev GCATGAAGAGGAAGGTCAGATAG, nested Fw CTTCGCTCATCGCCTTATCA, Rev ATGCTGTGTGGCAGATGAA.

Affymetrix Mouse Microarray analyses

For RNA expression in mouse PTGs, four batches of glands (PTGs) were dissected free of thyroid and the surrounding fibrous tissues and used for RNA extraction with a RNA-Stat 60 kit (Thermo Fisher Scientific, Inc.) as described previously (25). The RNA was reversed transcribed into cDNA, which was then subjected to Affymetrix Mouse GeneChip Microarray analyses by the Genome Technologies Core Facility (University of Manchester) and Genome Analyses Microarray Core (University of California San Francisco). The gene array data were analyzed using Affymetrix Genechip Software for an intensity value and normalized and presented as % of the expression level of a mitochondrial microsomal protein L19 (L19) and used for statistical analyses. n=4 batches of RNA with each batch extracted from 20 PTGs dissected from 10 of 6-week-old C57bB6 mice.

Co-immunoprecipitation

PTH-C1 or HEK293T cells were lysed in native lysis solution (1% Triton, 150 mM NaCl, 10 mM Tris-HCl, pH. 7.5, 1 mM EDTA, 1 mM EGTA, 0.5% Igepal, 10 % sucrose, 5mM NaF, 200uM vanadate, protease inhibitor) in 4°C for 30 min. Cleared lysates were collected and used for co-immunoprecipitations. Myc- or GST-tagged proteins were captured using a rabbit monoclonal antibody against myc tag (Clone 71D10, Cell Signaling, 2278) or Glutathione Sepharose 4B (GE Healthcare, GE17-0756-01), respectively. TRPC1 was detected using 1F1 (51), Gαs (Santa Cruz sc-135914), or GST (Santa Cruz, sc-459). Gα11 was detected using FLAG antibody (Clone M2, Sigma, F1804).

Immunohistochemistry staining for mouse PTG

Four micron thick histological sections, embedded in paraffin and mounted on HistoBond®Plus slides (Statlab Medical Products, Lewisville, TX) were rehydrated and washed in Tris Buffered Saline (TBS). The sections were processed for Immunohistochemistry using the M.O.M (Mouse on Mouse ImmPRESS

Peroxidse Polymer kit, Vector Labs, Inc, Burlingame, CA) or for rabbit antibodies the ImmPRESS –VR Horse Anti-Rabbit IgG Polymer Peroxidase kit (Vector Labs Inc., Burlingame CA). Antigen retrieval (pH 6 Citrate Antigen Unmasking Solution, Vector Labs Inc., Burlingame,CA) was accomplished via 20 min in a steamer followed by 30 min cooling at room temperature. Sections were treated with a peroxidase blocking reagent (Bloxall, Vector Laboratories, Inc, Burlingame, CA)

Double indirect immunofluorescence labeling

PTH-C1 and PTH-C1$^{Trpc1\text{-}KO}$ cells seeded on coverslips were fixed with cold methanol for 5 min in room temperature and then washed 3 times with ice cold PBS. Cells were permeabilized with 0.5% Saponin solution for 10 min followed by 3 washes in PBS. Blocking was done with 3% BSA for 15 min and then cells were incubated with primary antibody (TRPC1-1F1 1:500, Gα11 1:200) diluted in 1% BSA in 4° C overnight. Secondary antibodies coupled to Alexa Fluor® 488 (ThermoFisher, A11029 used at 1:2,000 dilution) or Alexa Fluor® 594 (ThermoFisher, A11012 used at 1:2,000 dilution) were added on coverslips for 2h in 4° C followed by 3 washes in PBS. Coverslips were mounted with Diamond DAPI solution (ThermoFisher ProLong™ Diamond Antifade Mountant with DAPI, P36962). Images were acquired and processed with laser scanning confocal microscope (Olympus Fluoview 1000), in an inverted configuration.

Statistics

All experiments showing protein-protein interactions and indirect immunofluorescence staining were repeated at least three times. Data measurements were presented as mean value ± standard error (SE). Difference between two groups was determined by unpaired, two-tailed Student's t-test or Mann Whitney test (if data within groups fail to show normal distribution as determined by the D'Agostino & Pearson

normality test). Significant difference between more than two groups was determined by one or two-way ANOVA, as indicated followed by Sidak's multiple comparison test or Kruskal-Wallis test followed by Dunn's multiple comparison test (if data failed the D'Agostino & Pearson normality test). All statistical analyses were performed in GraphPad Prism 7 software. *p<0.05, **p<0.01, ***p<0.001, ****p<0.0001.

To establish whether our analysis was sufficiently powered to detect at least one *TRPC1* mutation with a greater than 95% likelihood, the sample size required was determined by binomial probability analysis (Microsoft Excel), as previously reported (24). Approximately 65% of FHH1 patients have a *CASR* mutation (52), and for this binomial analysis the prevalence for *TRPC1* mutations in FHH patients without *CASR*, *GNA11* or *AP2S1* mutations was set at 20%, and a similar approach to that described for a search of *AP2S1* mutations in ADH patients was utilized (24). The binomial distribution probability was calculated using the following formula: Binomial distribution probability=b(x;n,p), where b(x;n,p)=(nx)px(1−p)n−x where n = sample size, x = number of probands harboring mutations; n-x = number of probands with no mutation; and p = prevalence of *TRPC1* mutations in the cohort.

Study approval

Animal studies described in this manuscript were approved by the OUHSC IACUC (301163 OUHSC IACUC Original Protocol Approval_18-101_11/7/2018#18-101) on 11/7/2018, as shown below:

Available:
Mouse #1
D: 3160

The above mentioned protocol was reviewed and approved by the Institutional Animal Care and Use Committee.

Prior to starting your animal studies, please ensure that the following is completed:

- HAZARDOUS MATERIALS: Investigators that plan to work with new hazards (chemical or infectious) should arrange to meet with a Comparative Medicine (CM) facility manager prior to the commencement of work involving new hazardous materials.

- SURGICAL PROCEDURES: Investigators that plan to perform new surgical procedures should notify a program veterinarian within Comparative Medicine or OAWA prior to the commencement of novel surgical procedures.

Review of IACUC Policies and SOPs
Researchers and personnel must familiarize themselves with applicable IACUC policies, procedures, and guidelines. These documents can be accessed at https://acup.ouhsc.edu/.

Unexpected Experimental Outcomes
Any unexpected experimental and non-experimental outcome must be reported to the IACUC via the Office of Animal Welfare Assurance (OAWA). IACUC policies describing these requirements may be found at: https://acup.ouhsc.edu/policies.html.

Protocol Modifications
Any changes to the approved protocol (e.g., personnel, procedures, animal numbers) must be reviewed and approved by the IACUC prior to being implemented. Additional information on the protocol review process can be found at: https://acup.ouhsc.edu/protocol-development.html.

The required form for submitting amendment requests is available at http://topaz.ouhsc.edu/topazelements/.

Protocol Expiration
Protocols have a lifespan of three (3) years. In order to continue projects beyond the three year protocol lifespan, a replacement protocol (de novo) must be reviewed and approved by the IACUC BEFORE the original protocol expires.

You will be notified at least 90 days prior to the expiration date of the protocol. It is the investigator's responsibility to submit a replacement (de novo) protocol in time for it to be reviewed and approved by the IACUC before original protocol expires. If a replacement protocol is approved please go to https://acup.ouhsc.edu/forms.html to transfer animals to the new protocol. If animals are assigned to an expiring protocol without an authorized transfer request in place, all research activities related to the expired protocol must stop, including breeding and studies in progress. No new animals may be ordered onto an expiring protocol. Any animal experimentation that is carried out under an expired protocol will be considered a major violation of federal regulations and will be reported to the granting agency, the NIH Office of Laboratory Animal Welfare (OLAW), and the U.S. Department of Agriculture (USDA) Animal and Plant Health Inspection Service (APHIS) if the animals are those species regulated by the USDA.

Sincerely
Eric Howard, Ph.D.
Chairman, Institutional Animal Care and Use Committee

Author contributions

MO, VN, and LT performed and analyzed *in vitro* experiments. MO, PN, BE, and KL performed and analyzed *in vivo* experiments. MO, MBH, and WC performed *ex vivo* experiments. ML performed immunohistochemistry staining studies. MLB provided critical reagents. CMG, VJS, and RVT performed and analyzed data on DNA sequencing of human samples. MO and LT wrote the manuscript with the help of MBH and KL. LT oversaw the project.

Acknowledgments

This work was supported by: grants from NIH R01AR064211 (LT and MBH), Presbyterian Health Foundation (MBH), NIH R01DK12165601 (LT and WC), VA-BLR&D I01BX003453 (WC), F.I.R.M.O. Foundation (MLB), Wellcome Trust Investigator Award (RVT), and a Welcome Trust Clinical Training Fellowship (VJS). We thank Drs. Mark Stevenson (University of Oxford, UK) for assistance in the analysis of human DNA sequencing data and Donald Ward (University of Manchester, UK) and Arthur Conigrave (University of Sydney, Australia) for assistance in initial Affymetrix Microarray Analyses.

References

1. Pollak MR, Seidman CE, and Brown EM. Three inherited disorders of calcium sensing. *Medicine.* 1996;75(3):115-23.
2. Pollak MR, Brown EM, Chou YH, Hebert SC, Marx SJ, Steinmann B, et al. Mutations in the human Ca(2+)-sensing receptor gene cause familial hypocalciuric hypercalcemia and neonatal severe hyperparathyroidism. *Cell.* 1993;75(7):1297-303.
3. Nesbit MA, Hannan FM, Howles SA, Babinsky VN, Head RA, Cranston T, et al. Mutations affecting G-protein subunit alpha11 in hypercalcemia and hypocalcemia. *N Engl J Med.* 2013;368(26):2476-86.
4. Nesbit MA, Hannan FM, Howles SA, Reed AA, Cranston T, Thakker CE, et al. Mutations in AP2S1 cause familial hypocalciuric hypercalcemia type 3. *Nat Genet.* 2013;45(1):93-7.
5. Lee JY, and Shoback DM. Familial hypocalciuric hypercalcemia and related disorders. *Best practice & research Clinical endocrinology & metabolism.* 2018;32(5):609-19.
6. Hannan FM, Kallay E, Chang W, Brandi ML, and Thakker RV. The calcium-sensing receptor in physiology and in calcitropic and noncalcitropic diseases. *Nature reviews Endocrinology.* 2018;15(1):33-51.
7. Shoback DM, Thatcher J, Leombruno R, and Brown EM. Relationship between parathyroid hormone secretion and cytosolic calcium concentration in dispersed bovine parathyroid cells. *Proc Natl Acad Sci U S A.* 1984;81(10):3113-7.
8. Hannan FM, and Thakker RV. Calcium-sensing receptor (CaSR) mutations and disorders of calcium, electrolyte and water metabolism. *Best practice & research Clinical endocrinology & metabolism.* 2013;27(3):359-71.
9. Conigrave AD. The Calcium-Sensing Receptor and the Parathyroid: Past, Present, Future. *Frontiers in physiology.* 2016;7:563.
10. Prakriya M, and Lewis RS. Store-Operated Calcium Channels. *Physiol Rev.* 2015;95(4):1383-436.
11. Clapham DE. TRP channels as cellular sensors. *Nature.* 2003;426(6966):517-24.
12. Venkatachalam K, and Montell C. TRP channels. *Annu Rev Biochem.* 2007;76:387-417.
13. Nesin V, and Tsiokas L. TRPC1. *Handbook of experimental pharmacology.* 2014;222:15-51.
14. Greenberg HZE, Carlton-Carew SRE, Khan DM, Zargaran AK, Jahan KS, Vanessa Ho WS, et al. Heteromeric TRPV4/TRPC1 channels mediate calcium-sensing receptor-induced nitric oxide production and vasorelaxation in rabbit mesenteric arteries. *Vascular pharmacology.* 2017;96-98:53-62.
15. Rey O, Young SH, Jacamo R, Moyer MP, and Rozengurt E. Extracellular calcium sensing receptor stimulation in human colonic epithelial cells induces intracellular calcium oscillations and proliferation inhibition. *J Cell Physiol.* 2010;225(1):73-83.
16. Rey O, Young SH, Papazyan R, Shapiro MS, and Rozengurt E. Requirement of the TRPC1 cation channel in the generation of transient Ca2+ oscillations by the calcium-sensing receptor. *J Biol Chem.* 2006;281(50):38730-7.

17. Qu YY, Wang LM, Zhong H, Liu YM, Tang N, Zhu LP, et al. TRPC1 stimulates calciumsensing receptorinduced storeoperated Ca2+ entry and nitric oxide production in endothelial cells. *Molecular medicine reports.* 2017;16(4):4613-9.
18. El Hiani Y, Ahidouch A, Lehen'kyi V, Hague F, Gouilleux F, Mentaverri R, et al. Extracellular signal-regulated kinases 1 and 2 and TRPC1 channels are required for calcium-sensing receptor-stimulated MCF-7 breast cancer cell proliferation. *Cellular physiology and biochemistry : international journal of experimental cellular physiology, biochemistry, and pharmacology.* 2009;23(4-6):335-46.
19. Dietrich A, Kalwa H, Storch U, Mederos YSM, Salanova B, Pinkenburg O, et al. Pressure-induced and store-operated cation influx in vascular smooth muscle cells is independent of TRPC1. *Pflugers Arch.* 2007;455(3):465-77.
20. Jakobsen NF, Rolighed L, Moser E, Nissen PH, Mosekilde L, and Rejnmark L. Increased trabecular volumetric bone mass density in Familial Hypocalciuric Hypercalcemia (FHH) type 1: a cross-sectional study. *Calcified tissue international.* 2014;95(2):141-52.
21. Christensen SE, Nissen PH, Vestergaard P, Heickendorff L, Rejnmark L, Brixen K, et al. Skeletal consequences of familial hypocalciuric hypercalcaemia vs. primary hyperparathyroidism. *Clinical endocrinology.* 2009;71(6):798-807.
22. Cheng Z, Liang N, Chen TH, Li A, Santa Maria C, You M, et al. Sex and age modify biochemical and skeletal manifestations of chronic hyperparathyroidism by altering target organ responses to Ca2+ and parathyroid hormone in mice. *J Bone Miner Res.* 2013;28(5):1087-100.
23. Ong EC, Nesin V, Long CL, Bai CX, Guz JL, Ivanov IP, et al. A TRPC1 Protein-dependent Pathway Regulates Osteoclast Formation and Function. *J Biol Chem.* 2013;288(31):22219-32.
24. Rogers A, Nesbit MA, Hannan FM, Howles SA, Gorvin CM, Cranston T, et al. Mutational analysis of the adaptor protein 2 sigma subunit (AP2S1) gene: search for autosomal dominant hypocalcemia type 3 (ADH3). *The Journal of clinical endocrinology and metabolism.* 2014;99(7):E1300-5.
25. Chang W, Tu C, Chen TH, Bikle D, and Shoback D. The extracellular calcium-sensing receptor (CaSR) is a critical modulator of skeletal development. *Sci Signal.* 2008;1(35):ra1.
26. Fabbri S, Ciuffi S, Nardone V, Gomes AR, Mavilia C, Zonefrati R, et al. PTH-C1: a rat continuous cell line expressing the parathyroid phenotype. *Endocrine.* 2014;47(1):90-9.
27. Rubaiy HN, Ludlow MJ, Henrot M, Gaunt HJ, Miteva K, Cheung SY, et al. Picomolar, selective, and subtype-specific small-molecule inhibition of TRPC1/4/5 channels. *J Biol Chem.* 2017;292(20):8158-73.
28. Kim MS, Zeng W, Yuan JP, Shin DM, Worley PF, and Muallem S. Native Store-operated Ca2+ Influx Requires the Channel Function of Orai1 and TRPC1. *J Biol Chem.* 2009;284(15):9733-41.
29. Nesin V, Wiley G, Kousi M, Ong EC, Lehmann T, Nicholl DJ, et al. Activating mutations in STIM1 and ORAI1 cause overlapping syndromes of tubular myopathy and congenital miosis. *Proc Natl Acad Sci U S A.* 2014;111(11):4197-202.
30. Parekh AB, and Putney JW, Jr. Store-operated calcium channels. *Physiol Rev.* 2005;85(2):757-810.
31. Obukhov AG, Harteneck C, Zobel A, Harhammer R, Kalkbrenner F, Leopoldt D, et al. Direct activation of trpl cation channels by G alpha11 subunits. *Embo J.* 1996;15(21):5833-8.
32. Chang W, and Shoback D. Extracellular Ca2+-sensing receptors--an overview. *Cell Calcium.* 2004;35(3):183-96.
33. Brown EM, Pollak M, and Hebert SC. The extracellular calcium-sensing receptor: its role in health and disease. *Annu Rev Med.* 1998;49:15-29.
34. Christensen SE, Nissen PH, Vestergaard P, Heickendorff L, Rejnmark L, Brixen K, et al. Plasma 25-hydroxyvitamin D, 1,25-dihydroxyvitamin D, and parathyroid hormone in familial hypocalciuric hypercalcemia and primary hyperparathyroidism. *European journal of endocrinology.* 2008;159(6):719-27.

35. Christensen SE, Nissen PH, Vestergaard P, and Mosekilde L. Familial hypocalciuric hypercalcaemia: a review. *Current opinion in endocrinology, diabetes, and obesity.* 2011;18(6):359-70.
36. Vargas-Poussou R, Mansour-Hendili L, Baron S, Bertocchio JP, Travers C, Simian C, et al. Familial Hypocalciuric Hypercalcemia Types 1 and 3 and Primary Hyperparathyroidism: Similarities and Differences. *The Journal of clinical endocrinology and metabolism.* 2016;101(5):2185-95.
37. Davies M, Adams PH, Berry JL, Lumb GA, Klimiuk PS, Mawer EB, et al. Familial hypocalciuric hypercalcaemia: observations on vitamin D metabolism and parathyroid function. *Acta endocrinologica.* 1983;104(2):210-5.
38. Law WM, Jr., Bollman S, Kumar R, and Heath H, 3rd. Vitamin D metabolism in familial benign hypercalcemia (hypocalciuric hypercalcemia) differs from that in primary hyperparathyroidism. *The Journal of clinical endocrinology and metabolism.* 1984;58(4):744-7.
39. Szalat A, Shpitzen S, Tsur A, Zalmon Koren I, Shilo S, Tripto-Shkolnik L, et al. Stepwise CaSR, AP2S1, and GNA11 sequencing in patients with suspected familial hypocalciuric hypercalcemia. *Endocrine.* 2017;55(3):741-7.
40. Toka HR, Al-Romaih K, Koshy JM, DiBartolo S, 3rd, Kos CH, Quinn SJ, et al. Deficiency of the calcium-sensing receptor in the kidney causes parathyroid hormone-independent hypocalciuria. *J Am Soc Nephrol.* 2012;23(11):1879-90.
41. Kristiansen JH, Rodbro P, Christiansen C, Johansen J, and Jensen JT. Familial hypocalciuric hypercalcaemia. III: Bone mineral metabolism. *Clinical endocrinology.* 1987;26(6):713-6.
42. Ho C, Conner DA, Pollak MR, Ladd DJ, Kifor O, Warren HB, et al. A mouse model of human familial hypocalciuric hypercalcemia and neonatal severe hyperparathyroidism. *Nat Genet.* 1995;11(4):389-94.
43. Howles SA, Hannan FM, Gorvin CM, Piret SE, Paudyal A, Stewart M, et al. Cinacalcet corrects hypercalcemia in mice with an inactivating Galpha11 mutation. *JCI insight.* 2017;2(20).
44. Offermanns S, Zhao LP, Gohla A, Sarosi I, Simon MI, and Wilkie TM. Embryonic cardiomyocyte hypoplasia and craniofacial defects in G alpha q/G alpha 11-mutant mice. *Embo j.* 1998;17(15):4304-12.
45. Wettschureck N, Lee E, Libutti SK, Offermanns S, Robey PG, and Spiegel AM. Parathyroid-specific double knockout of Gq and G11 alpha-subunits leads to a phenotype resembling germline knockout of the extracellular Ca2+ -sensing receptor. *Molecular endocrinology (Baltimore, Md.* 2007;21(1):274-80.
46. Wes PD, Chevesich J, Jeromin A, Rosenberg C, Stetten G, and Montell C. TRPC1, a human homolog of a Drosophila store-operated channel. *Proc Natl Acad Sci U S A.* 1995;92(21):9652-6.
47. Stormorken H. [Stormorken's syndrome]. *Tidsskr Nor Laegeforen.* 2002;122(30):2853-6.
48. Myeong J, Ko J, Kwak M, Kim J, Woo J, Ha K, et al. Dual action of the Galphaq-PLCbeta-PI(4,5)P2 pathway on TRPC1/4 and TRPC1/5 heterotetramers. *Scientific reports.* 2018;8(1):12117.
49. Zheng W, Cai R, Hofmann L, Nesin V, Hu Q, Long W, et al. Direct Binding between Pre-S1 and TRP-like Domains in TRPP Channels Mediates Gating and Functional Regulation by PIP2. *Cell reports.* 2018;22(6):1560-73.
50. Reiniger N, Lau K, McCalla D, Eby B, Cheng B, Lu Y, et al. Deletion of the receptor for advanced glycation end products reduces glomerulosclerosis and preserves renal function in the diabetic OVE26 mouse. *Diabetes.* 2010;59(8):2043-54.
51. Ma R, Rundle D, Jacks J, Koch M, Downs T, and Tsiokas L. Inhibitor of myogenic family, a novel suppressor of store-operated currents through an interaction with TRPC1. *J Biol Chem.* 2003;278(52):52763-72.
52. Hannan FM, Babinsky VN, and Thakker RV. Disorders of the calcium-sensing receptor and partner proteins: insights into the molecular basis of calcium homeostasis. *Journal of molecular endocrinology.* 2016;57(3):R127-42.

Figure 1

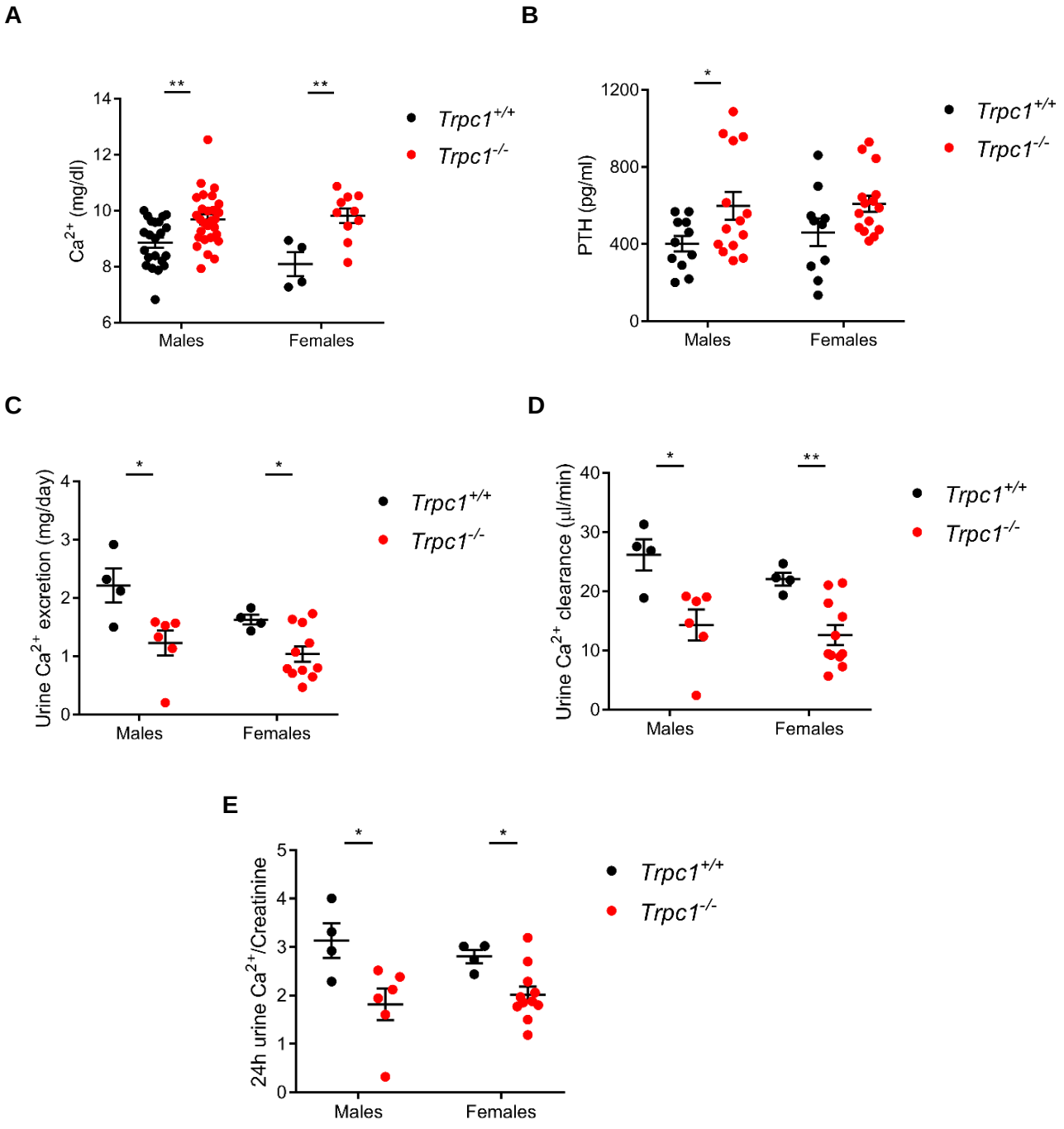

Fig. 1 *Trpc1*$^{-/-}$ mice exhibit hypercalcemia, hyperparathyroidism, and hypocalciuria.

A) Serum Ca^{2+} levels (mg/dl) in 7 month-old *Trpc1*$^{+/+}$ and *Trpc1*$^{-/-}$ fasted males and females. **, p<0.01, Student's t test.

B) Serum PTH levels (pg/ml) in 7 month-old *Trpc1*$^{+/+}$ and *Trpc1*$^{-/-}$ fasted males and females. *, p<0.05, Student's t test.

C) Urine Ca^{2+} excretion (mg/day) in 7 month-old *Trpc1*$^{+/+}$ and *Trpc1*$^{-/-}$ males and females. *, $p<0.05$, Student's t test.
D) Ca^{2+} clearance (μl/min) in 7 month-old *Trpc1*$^{+/+}$ and *Trpc1*$^{-/-}$ males and females. *, $p<0.05$; **, $p<0.01$, Student's t test.
E) Twenty-four hour urine Ca^{2+}/creatinine ratio in 7 month-old *Trpc1*$^{+/+}$ and *Trpc1*$^{-/-}$ males and females. *, $p<0.05$, Student's t test.

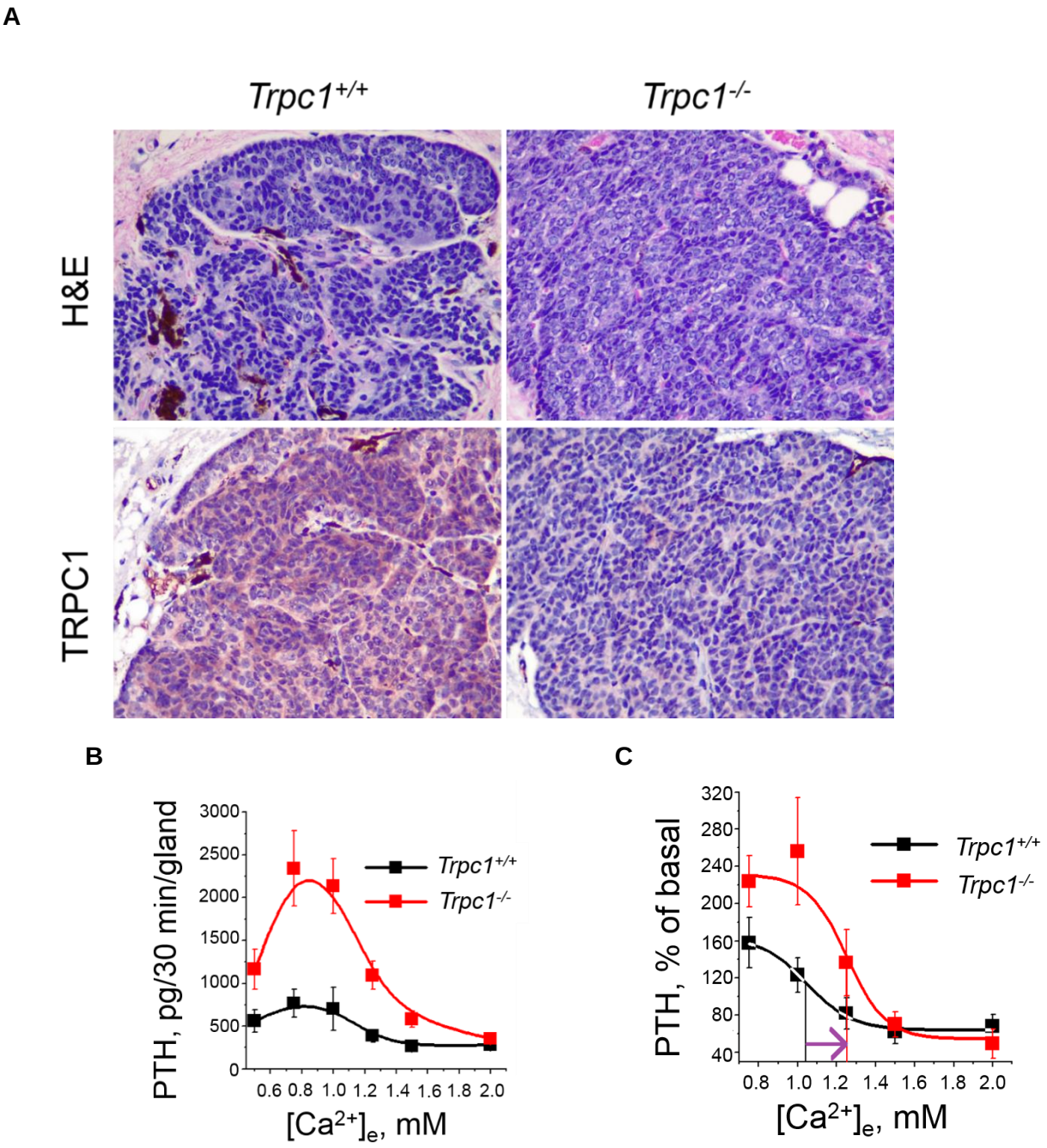

Figure 2. Parathyroid glands lacking TRPC1 fail to properly control PTH secretion.

A) TRPC1 is widely expressed in normal mouse PTGs. Top panels: H&E staining of *Trpc1*$^{+/+}$ (left) and *Trpc1*$^{-/-}$ (right) glands. Bottom panels: Expression of TRPC1 in wild type (left) and *Trpc1*-null (right) PTGs by immunohistochemistry using a mouse monoclonal antibody against TRPC1 (1F1). Magnification: 40X.

B) Responses of PTH release at different $[Ca^{2+}]_e$ (pg/30 min/gland) in PTGs isolated from 8 (3 males and 5 females) WT and 8 (3 males and 5 females) 14 week-old *Trpc1*-null mice.
C) Ca^{2+} dose-response curves shown in (B) were normalized and expressed as % of the PTH release at 0.5 mM Ca^{2+}. Perpendicular lines depict Ca^{2+} set points (1.04 ± 0.15 for *Trpc1*$^{+/+}$ and 1.25 ± 0.08 for *Trpc1*$^{-/-}$ mice).

Figure 3

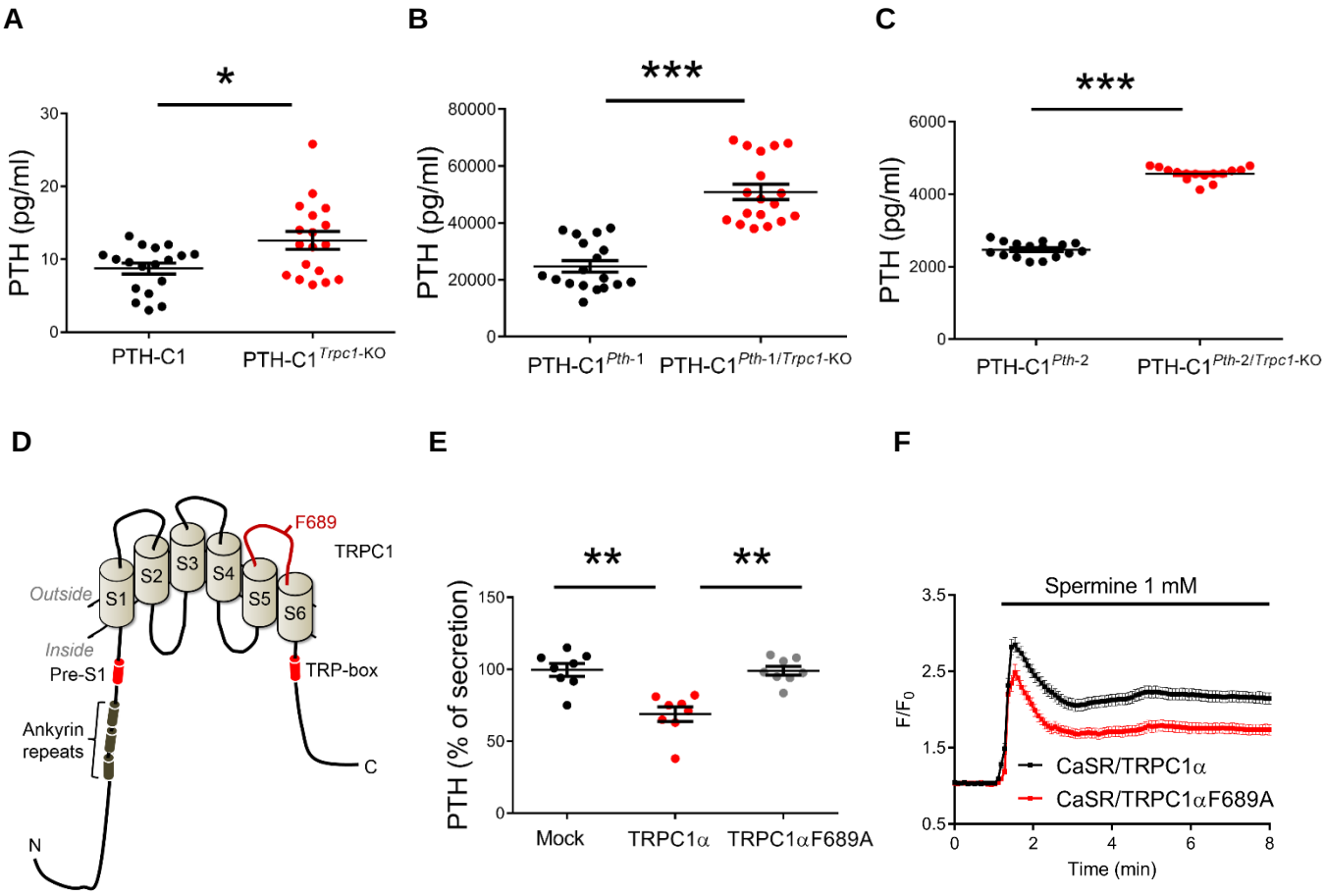

Figure 3 Inactivation of the *Trpc1* gene increases PTH secretion.

(A-C) Absolute PTH levels in media of wild type PTH-C1 cells, or cells lacking TRPC1 in the presence or absence of exogenously transfected PTH. *, p<0.05; ***, p<0.001, Student's t test.

D) TRPC1 topology and location of F689. Pore-forming region connecting S5 and S6 is shown in red. Ankyrin repeats are shown as dark green cylinders and Pre-S1 and TRP-box domains as shown are red cylinders.

E) Re-addition of wild type mouse TRPC1α, but not the TRPC1αF689A pore mutant rescues suppressed PTH secretion in cells lacking endogenous rat TRPC1 (PTH-C1$^{PTH\text{-}2/Trpc1\text{-}KO}$) cells. Data from 9-18 measurements were pooled from 3-6 independent experiments. *, p<0.05; **, p<0.01. One-way ANOVA.

F) Spermine-induced changes in free intracellular Ca^{2+} in HEK293 cells transiently co-transfected with CaSR plus wild type TRPC1α (black, n=296 cells pooled from 3 experiments) or TRPC1α-F689A (red, n=276 cells pooled from 3 experiments).

Figure 4

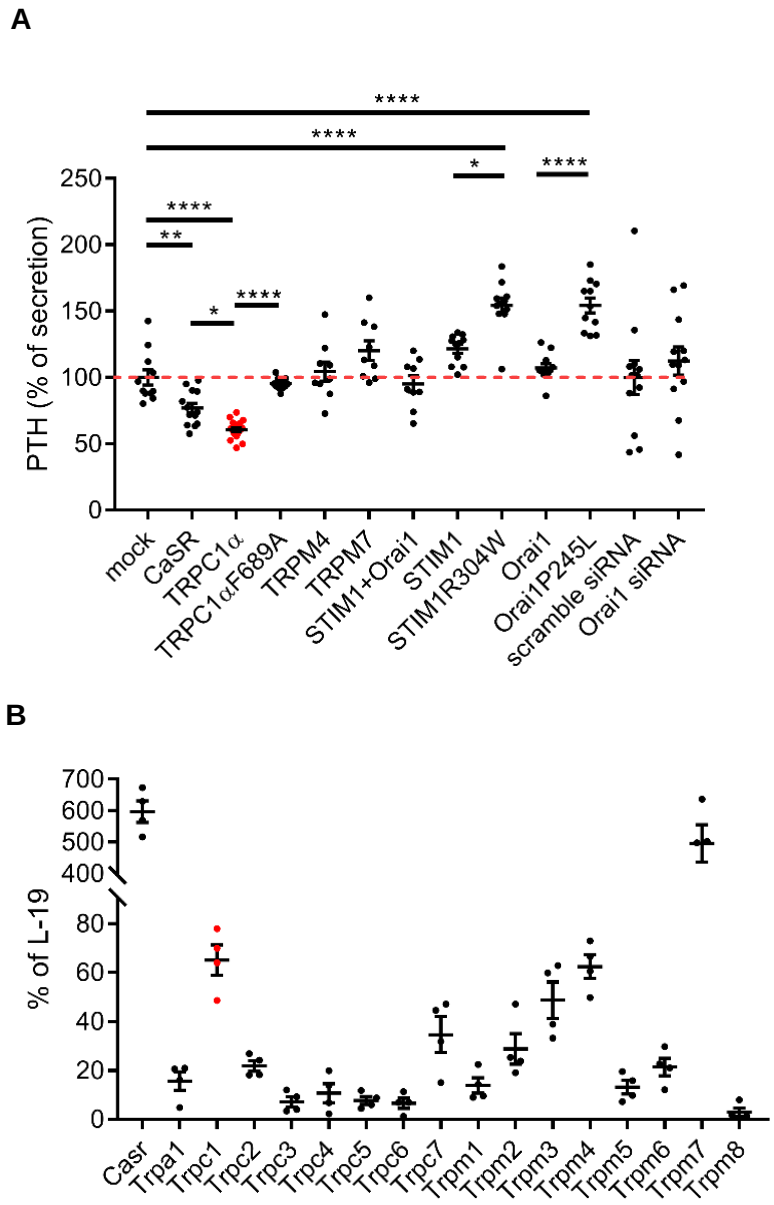

Figure 4 TRPC1 overexpression suppresses PTH secretion independently of SOCE and other TRP channels expressed in the mouse PTG.

(A) Normalized levels of secreted PTH in media of PTH-C1 cells transiently transfected indicated expression plasmids or siRNAs (n=9 measurements pooled from 3 independent experiments). *, p<0.05; **, p<0.005; ***,p<0.001, ****, p<0.0001. One-way ANOVA.

(B) Expression levels of TRP channel mRNAs in mouse PTG by Affymetrix Mouse Microarray analyses. L-19 was used as the house-keeping gene (n=4 batches of 20 PTGs).

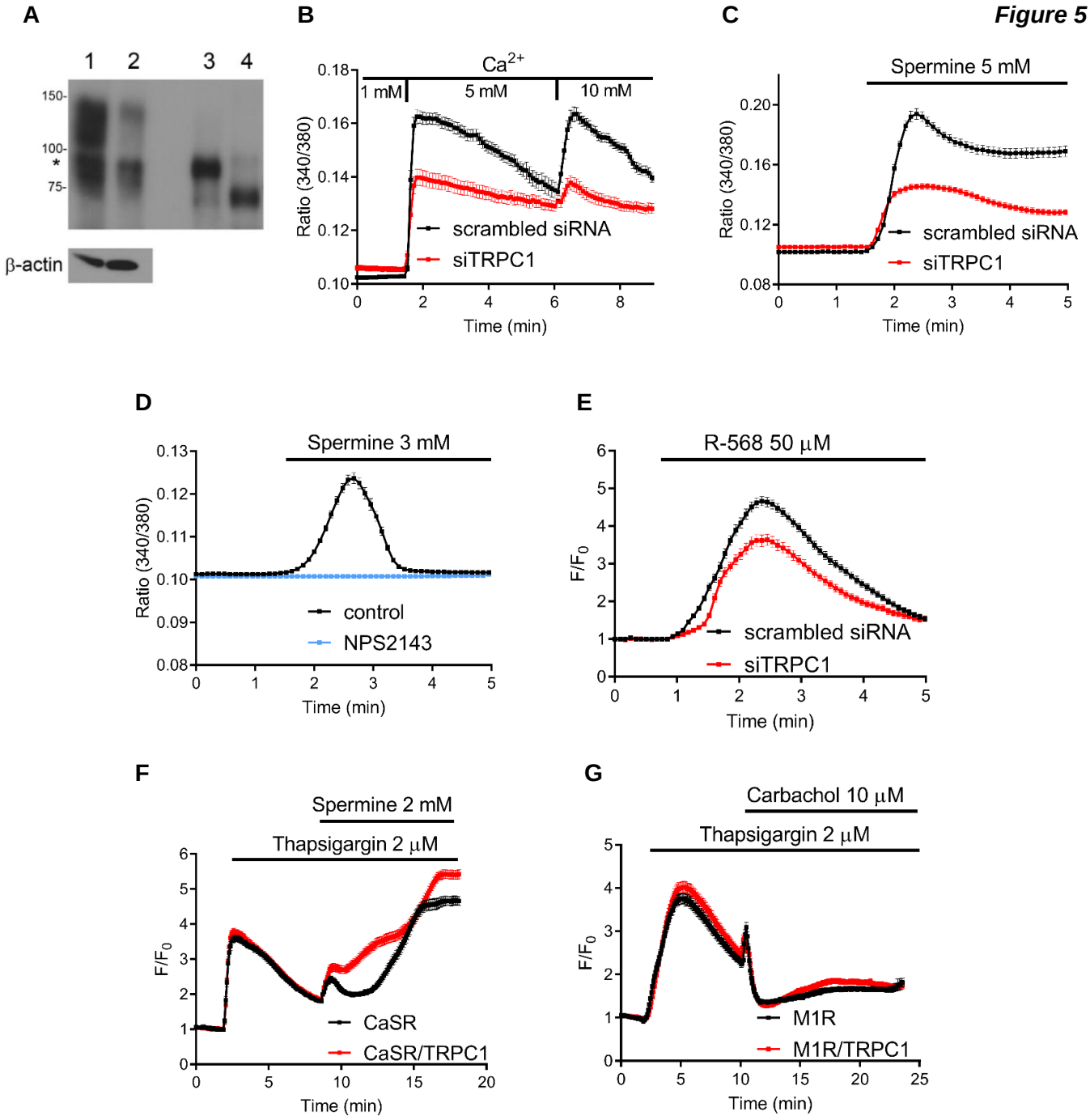

Figure 5 TRPC1 is required for CaSR-induced Ca^{2+} signaling in PTH-C1 cells.

(A) Efficiency of TRPC1 knockdown using RNAi. PTH-C1 cells were transiently transfected with a scrambled siRNA (lane 1), siTRPC1 (lane 2), expression plasmid (positive control) of a long-form of TRPC1α (lane 3) or a short-form of TRPC1α (lane 4). TRPC1 was immunoprecipitated and immunoblotted with a TRPC1-specific monoclonal antibody (1F1). PTH-C1 cells express predominantly the long form of TRPC1α (indicated by an asterisk).

(B) Changes in intracellular Ca^{2+} concentration (expressed as fluorescence ratio 340/380) in PTH-C1 cells transiently transfected with a scrambled siRNA (control, black, n=76 cells pooled from 5 independent experiments) or a *Trpc1*-specific siRNA (siTRPC1, red, n=61 cells pooled from 6 independent experiments) and cultured in 1, 5, or 10 mM of extracellular Ca^{2+}.

(C) Time-course of Spermine (5 mM)-induced intracellular Ca^{2+} concentration in PTH-C1 cells transiently transfected with a scrambled siRNA (control, black, n=144 cells pooled from 4 independent experiments) or a *Trpc1*-specific siRNA (siTRPC1, red, n=178 cells pooled from 8 independent experiments).

(D) Time-course of intracellular Ca^{2+} concentration in PTH-C1 cells cultured in zero extracellular Ca^{2+} and activated by Spermine (3 mM) in the presence (blue, n=279 cells from 6 experiments) or absence of NPS2143 (300 nM) (black, n=233 cells from 5 experiments).

(E) Time-course of R568 (50 μM)-induced intracellular Ca^{2+} concentration in PTH-C1 cells transiently co-transfected with GCaMP3 and scrambled siRNA (control, black line, n=216 cells pooled from 9 independent experiments) or TRPC1 siRNA (siTRPC1, red line, n=172 cells pooled from 9 independent experiments) in the presence of 1.8 mM extracellular Ca^{2+} concentration. F_0 was the average fluorescence for 1 min prior to the addition of R-568.

(F, G) TRPC1 is specifically coupled to CaSR. HEK293 cells were transiently co-transfected with GCaMP3, CaSR (F) or m1 muscarinic acetylcholine receptor (m1 AchR, G) in the presence or absence of TRPC1 (red or black traces). Cells were first stimulated with thapsigargin (2μM) to deplete the internal stores and then with Spermine (2 mM, F) or Carbachol (10μM, G) to activate CaSR or m1 AchR, respectively. Changes in intracellular free Ca^{2+} concentration are reported as F/F_0. Data were pooled from 6 independent experiments totaling 263 cells transfected with CaSR (black, F) and 316 cells transfected with CaSR plus TRPC1 (red, F) or from 8 independent experiments totaling 190 cells transfected with m1 AchR (black, G) and 173 cells transfected with m1 AchR plus TRPC1 (red, G).

Figure 6

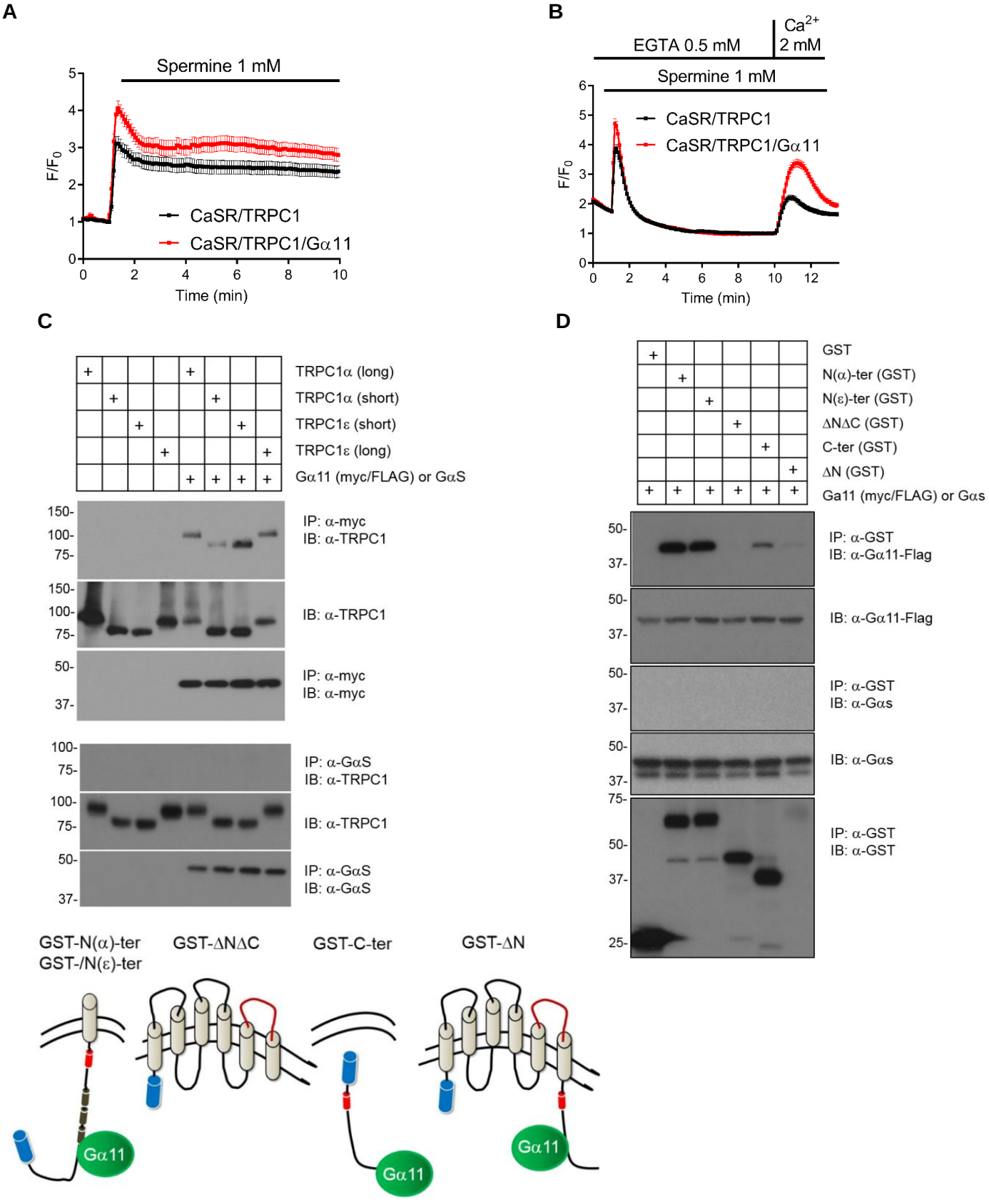
A
Spermine 1 mM
F/F0
Time (min)
CaSR/TRPC1
CaSR/TRPC1/Gα11
B
EGTA 0.5 mM
Ca2+ 2 mM
Spermine 1 mM
CaSR/TRPC1
CaSR/TRPC1/Gα11
F/F0
Time (min)
C
TRPC1α (long)
TRPC1α (short)
TRPC1ε (short)
TRPC1ε (long)
Gα11 (myc/FLAG) or GαS
IP: α-myc
IB: α-TRPC1
IB: α-TRPC1
IP: α-myc
IB: α-myc
IP: α-GαS
IB: α-TRPC1
IB: α-TRPC1
IP: α-GαS
IB: α-GαS
D
GST
N(α)-ter (GST)
N(ε)-ter (GST)
ΔNΔC (GST)
C-ter (GST)
ΔN (GST)
Ga11 (myc/FLAG) or Gαs
IP: α-GST
IB: α-Gα11-Flag
IB: α-Gα11-Flag
IP: α-GST
IB: α-Gαs
IB: α-Gαs
IP: α-GST
IB: α-GST
GST-N(α)-ter
GST-/N(ε)-ter
GST-ΔNΔC
GST-C-ter
GST-ΔN
Gα11
Gα11
Gα11

Figure 6 Gα11 physically interacts with TRPC1 and increases its activity

A and B) Gα11 increases TRPC1-mediated Ca^{2+} signaling in HEK293 cells. Cells were transiently transfected with CaSR and TRPC1α or CaSR, TRPC1α and Gα11. Both groups were co-transfected with the fluorescent Ca^{2+} indicator, GCaMP3, and fluorescence intensity was determined by single cell Ca^{2+} imaging. Changes in intracellular Ca^{2+} concentration (F/F_0) in response to Spermine (1 mM) were determined under physiological conditions (1.8 mM extracellular Ca^{2+}, B) or in Ca^{2+}-free extracellular solution followed by Ca^{2+} re-addition (2 mM, C). Data were pooled from 74 (black) or 85 (red) cells from 2 independent transfections (A) and 318 (black) or 261 (red) cells from 4 independent transfections (B).

C) HEK293T cells were transiently transfected with the long form of TRPC1ε, short form of TRPC1ε, short form of TRPC1α, long form of TRPC1α or the same TRPC1 plasmids plus myc-tagged Gα11 (upper three panels) or GαS (lower three panels). Gα11 was immunoprecipitated using α-myc, and GαS was immunoprecipitated using α-GαS. TRPC1 was detected in the complexes using anti-TRPC1 (upper panels). TRPC1 input is shown in middle panels and immunoprecipitated Gα11 or GαS is shown in lower panels.

D) Truncation mutants of TRPC1α (GST alone, GST-N(α)-ter, GST-N(ε)-ter, GST-ΔNΔC, GST-C-ter, GST-ΔN) shown in (D) tagged with GST (blue cylinders) were co-transfected with wild type Gα11 or Gαs. Protein-protein interactions were determined by GST-pulldowns followed by immunoblotting. Gα11 (first panel), but not Gαs (third panel) interacted with the cytosolic N- or C-tail of TRPC1. Gα11 input is shown in second panel, Gαs input is shown in fourth panel and immunoprecipitated mutants of TRPC1 are shown in lower panels.

Table 1

Parameter	Age (months)	*Trpc1*$^{+/+}$	*Trpc1*$^{-/-}$	*p* value
Serum Mg^{2+} (mg %)	7	0.83 ± 0.05 (n=16)	0.90 ± 0.03 (n=17)	ns
Serum Mg^{2+} (mg %)	16	0.97 ± 0.04 (n=36)	0.90 ± 0.03 (n=28)	ns
Urine Mg^{2+} excretion (mg/day)	7	1.8 ± 1.4 (n=4)	1.3 ± 2.2 (n=6)	ns
Mg^{2+} clearance (μl/min)	7	78 ± 3 (n=4)	54 ± 11 (n=6)	ns
24h urine Mg^{2+} / Creatinine	7	2.6 ± 0.5 (n=4)	1.9 ± 0.3 (n=6)	ns
Serum Phosphorous (mg %)	8	5.8 ± 0.3 (n=18)	6.4 ± 0.4 (n=14)	ns
Serum 1,25 $(OH)_2D_3$ (pg/ml)	7	308 ± 8 (n=11)	301 ± 5 (n=14)	ns
Serum Calcitonin (pg/ml)	7	22.3 ± 2.6 (n=11)	21.9 ± 2.2 (n=14)	ns
Serum Creatinine (mg/dl)	12	0.074 ± 0.005 (n=11)	0.083 ± 0.01 (n=10)	ns
24h urine creatinine clearance (ml/min/100 g body weight)	12	2.23 ± 0.23 (n=11)	2.18 ± 0.29 (n=10)	ns
Hematocrit (%)	8.5	52.7 ± 1.2 (n=12)	51.9 ± 2.3 (n=12)	ns
	10.5	58.5 ± 1.3 (n=11)	50.8 ± 1.3 (n=5)	<0.005
	21.5	56.2 ± 0.6 (n=8)	38.4 ± 1.8 (n=7)	<0.001

Table 1 Serum and urine analysis of biochemical parameters in *Trpc1*$^{+/+}$ and *Trpc1*$^{-/-}$ male mice.